JOURNAL OF Materials CHEMISTRY

Structural characterisations of a lamellar organic–inorganic nickel silicate obtained by hydrothermal synthesis from nickel acetate and (aminopropyl)triethoxysilane

Murielle Guillot, Mireille Richard-Plouet* and Serge Vilminot

IPCMS-GMI, UMR 7504, 23 Rue du Loess, Strasbourg 67037, France Cedex.
E-mail: richard@ipcms.u-strasbg.fr; Tel: 33 388 10 71 29

Received 8th November 2001, Accepted 2nd January 2002
First published as an Advance Article on the web 15th February 2002

Lamellar organic–inorganic nickel silicates have been synthesised under hydrothermal conditions at 170 °C from a mixture of nickel acetate solution and (aminopropyl)triethoxysilane. The influence of the presence or absence of a mineralising agent such as HF or NH_4F has been studied. Structural characterisations show that this material adopts a lamellar arrangement of nickel hydroxide layers separated by 21 Å with, in the interspace, organically modified silicate entities linked to the inorganic layer. The hysteresis cycle and ac susceptibility have been carried out and reveal a paramagnetic–ferromagnetic transition below 20 K.

Introduction

Much work deals with the synthesis of materials involving modified alkoxysilanes and transition metals.[1] One way to obtain these compounds is to precipitate with sodium hydroxide a suspension containing the transition metal salt and the organotrialkoxysilane in water + alcohol solution.[2–5] The authors are assuming that the structure is closely related to phyllosilicates. In these structures, divalent metals are in an octahedral coordination of oxygen atoms. The octahedra are connected by their edges to form a two dimensional divalent metal triangular array which is either bordered by one layer of silicate for 1 : 1 phyllosilicate (7 Å apart) or sandwiched by two layers of silicate for 2 : 1 phyllosilicate (9.4 Å apart). The silicon atoms are located in tetrahedral sites sharing all their corners. The solids obtained by precipitation present a low crystallinity characterised, in particular, by broad X-ray diffraction peaks.

Our group is involved in the synthesis of silicates under hydrothermal conditions. Thus some nickel silicates were obtained using tetraethyl orthosilicate leading to 1 : 1, $Ni_3Si_2O_5(OH)_{3.1}F_{0.9}$ and 2 : 1, $Ni_3Si_4O_{10}(OH)_{1.6}F_{0.4}$ structures. These compounds show a long range ferromagnetic order below 28 K, the easy magnetisation axis being perpendicular to the layers. In absence of any chemical bonds between the layers, dipolar interactions have been considered to take place, even for the 1 : 1 phyllosilicate with a 7 Å interlayer distance. In order to follow the influence of this distance on the magnetic properties, other samples have been prepared starting from a mixture of tetraethyl orthosilicate [$Si(OC_2H_5)_4$] and chemically modified silicon alkoxides, such as {3-[*N*-(2-aminoethyl)amino]propyl}trimethoxysilane [$H_2N(CH_2)_2NH(CH_2)_3Si(OCH_3)_3$] or {3-[*N*-(6-aminohexyl)amino]propyl}trimethoxysilane [$H_2N(CH_2)_6NH(CH_2)_3Si(OCH_3)_3$], yielding an increase up to 13.2 Å.[6] However, only a small amount of the alkyl substituted chain was still present in the lamellar compound. Moreover, we also suspected the formation of aminoalkyl cations unbonded to silicon. Therefore, an alkoxide with a smaller alkyl chain and only one amino group has been used, (3-aminopropyl)triethoxysilane [$H_2N(CH_2)_3Si(OC_2H_5)_3$]. The hydrothermal conditions have been optimised in order to use this alkoxide as the only source for silicon.

Experimental

Synthesis

From nickel acetate tetrahydrate, $Ni(CH_3COO)_2{\cdot}4H_2O$ (Aldrich, 98%) and (3-aminopropyl)triethoxysilane, APTES = $H_2N(CH_2)_3Si(OC_2H_5)_3$ (Fluka, 99%) with or without fluorine (HF, Merck 40% solution or NH_4F, Prolabo 98%) in respective proportions 3 : 4 : 215 : 0 or 1 treated under hydrothermal conditions. All reagents were used as received. Nickel acetate (3.807 g, 15 mmol) was dissolved in 20 ml deionized water containing HF (0.25 g, 5 mmol) or NH_4F (0.189 g, 5 mmol). The required quantity of APTES (4.466 g, 20 mmol) was weighed in a dry box and subsequently dropped into the nickel acetate aqueous solution under vigorous stirring. The resulting green suspension was aged for 3 hours and then heated in 125 ml Teflon lined reactors at 170 °C for 6 days. The solid was retrieved by centrifugation, redispersed in water, centrifuged again and dried at 100 °C in an oven. The compounds synthesised without fluorine, with NH_4F and HF are named samples 1, 2 and 3, respectively.

Imine formation: 200 mg of sample 2 and 40 mg *p*-nitrobenzaldehyde (Aldrich, 98%) were allowed to react in dried methanol under reflux at 60°C. Molecular sieves were introduced to trap water formed during the reaction. The material obtained was filtered and washed with methanol.

Characterisations

Air-dried products were examined by X-ray diffraction (XRD) on a Siemens D5000 diffractometer in a Bragg–Brentano geometry using Cu $K\alpha_1$ radiation (λ = 1.5406 Å).

Thermogravimetric (TGA) and differential thermal (DTA) analyses were performed, under air or argon, on a Setaram TGA 92 apparatus, using a 6 °C min^{-1} heating rate. A mass spectrometer was used to obtain information about the compounds evolved during heating.

For electron microscopy, samples were included in epoxy resin (EPON® 812, Fluka). Thin cuts were subsequently obtained with an ultramicrotome in order to observe samples perpendicularly to the layers. Observations were performed on a Topcon 002B microscope operating at a 200 kV accelerating voltage.

Infra-red spectra were recorded in transmission mode from

powder diluted in a dried KBr pellet, using an ATI Mattson spectrometer.

Hysteresis cycle at 2 K and AC susceptibility (in a 3.5 Oe field oscillating at 20 Hz) from 2 to 25 K were performed on a Quantum Design MPMS-XL SQUID magnetometer.

Chemical analyses were performed at the Service d'Analyse du CNRS de Vernaison by ICP technique.

XAS experimental

EXAFS measurements were performed at the Ni K-edge at the European Synchrotron Radiation Facilities (ESRF) at Grenoble, beam-line 29 (synchrotron current = 185 mA). The absorption coefficient was recorded at 50 K in transmission mode using two ionisation chambers (argon/air) for the detection. A Si (311) monochromator was used to cover the photon range from 8000 to 9500 eV with a 5 eV step during the pre-edge and across and 1 eV after edge. The elimination of the high order harmonics was assured *via* the double Si single crystal monochromator. No focusing mirror was used. Pellets were prepared by mixing each compound with the appropriate amount of boron nitride BN to obtain a close to 1 absorption jump across the edge. The Ni K-edge of $Ni(OH)_2$ was used for energy calibration. EXAFS measurements were recorded twice for each compound to get a good signal to noise ratio. Both reference samples, $Ni(OH)_2$ and 1 : 1 phyllosilicate $Ni_3Si_2O_5(OH)_4$ were also measured under the same conditions. They were chosen because in one case Ni is only surrounded by Ni atoms, as second neighbours, at 3.12 Å, whereas in the second case, there is a contribution of 2 Si at 3.24 Å in addition to the 6 Ni at 3.12 Å.

The $k\chi(k)$ function was extracted from the absorption coefficient using a cubic spline function.[7] E_0 was chosen at the very start of the jump, typically between 8378 and 8379 eV. The Fourier transforms were performed on $k^3\chi(k)$ with a Kaiser–Bessel window† (τ = 2.5) on the k-range 2–12 $Å^{-1}$. Using FEFF6 code[8] EXAFS oscillations were calculated for $Ni(OH)_2$ and $Ni_3Si_2O_5(OH)_4$ in order to have phases and amplitudes for the different shells: 6 oxygens as first neighbours, 6 Ni as second and 2 Si as third shell. Since peaks for the first, on the one hand, and second and third neighbours, on the other hand, are distinct on the Fourier transform, the inverse Fourier transforms were fitted independently using the software developed at LURE "Exafs pour le Mac".[7] The validity of this phase and amplitude was checked on the reference compounds before being applied to the hybrid samples as follows: the numbers of neighbours N_i were fixed for each shell and the other parameters of the EXAFS equation were refined, in the spherical waves theory, according to:

$$k\chi(k) = -S_o^2 \sum_i \frac{N_i}{R_i^2} |f_i(k,R_i)| e^{-2\sigma_i^2 k^2} e^{-2R_i/\lambda_i(k)} \sin(2kR_i + \phi_i(k,R_i))$$

where i is the number of the retrodiffusion shell, N_i the number of atoms at a distance R_i from the central Ni atom for each shell, σ_i the Debye–Waller factor, λ_i the mean free path, ϕ_i and f_i the phase and amplitude for the backscatters i. S_o^2 is the reduction factor (fixed to 1). Since the obtained distances and electronic parameters were correct, the hybrid compounds were fitted using the FEFF6 calculated phases and amplitudes for the different shells. The coordination numbers were fixed to 6 for oxygen first neighbours and 6 for Ni second neighbours. The goodness of the fit was assessed through the residue:

$$\rho = \frac{\sum_k (k\chi_{exp} - k\chi_{calc})^2}{\sum_k (k\chi_{exp})^2}$$

The statistical relevance was estimated with the fit quality factor

$$\chi_v^2 = \frac{\sum [k\chi_{th}(k) - k\chi_{exp}(k)]^2}{e^2 v}$$

with e the average experimental signal error and v the degree of freedom of the fit.

Results

X-Ray diffraction

After maturation, no X-ray diffraction peaks are noticeable even when the maturation time is increased. The higher the hydrothermal treatment temperature, the better is the crystallisation.

Whatever the conditions (with or without fluorine), a layered material (see scanning electron picture in Fig. 1) is always obtained with a characteristic pattern presented in Fig. 2. It represents a basal spacing close to 21 Å with several (00l) lines, up to l = 6. These reflections are rather broad (*ca.* 1.5° in 2θ). From the Scherrer formula, the coherent length along the stacking axis can be estimated to 10 nm. Taking into account a 21 Å interlayer distance, it means that only 6 layers are stacked coherently. This is obviously demonstrated on the high resolution transmission electron microscopy image (Fig. 3)

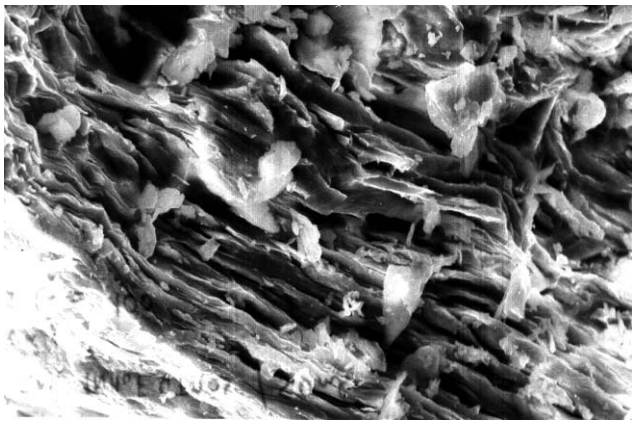

Fig. 1 Scanning electron microscopy of hybrid lamellar material (scale: 1 cm ≡ 15 μ).

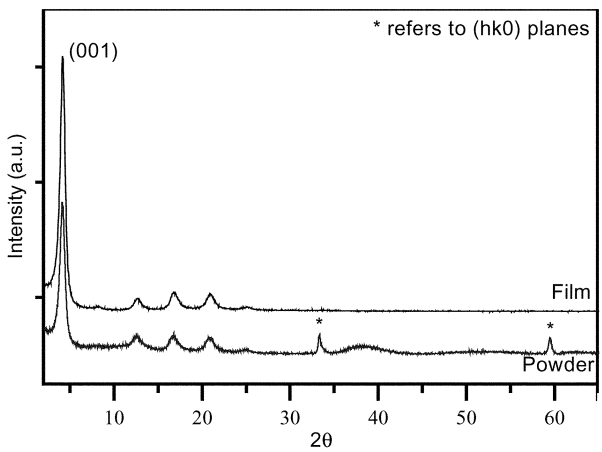

Fig. 2 XRD patterns of hybrid nickel silicate powder and film obtained after evaporation of silicate suspension on glass substrate.

†The FFT is performed on $\omega(k).k3.\chi(k)$ with

$$\omega(k) = \frac{I_O\left[\tau\sqrt{1-\left(\frac{2k-k_2-k_1}{k_2-k_1}\right)^2}\right]}{I_0(\tau)}$$

where k_1 and k_2 are the limits of the FFT, I_0 is the Bessel function.

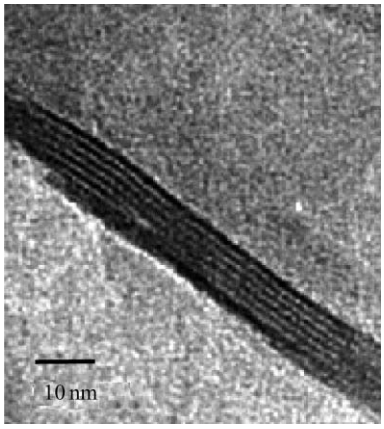

Fig. 3 Transmission electron microscopy image of lamellar crystal embedded in epoxy resin.

where only 6 layers are coherently stacked. The reflections at 2.67 and 1.54 Å are characteristic of intralayer (*hk*0) diffraction planes as usually observed in phyllosilicates or nickel hydroxide where Ni^{2+} ions are arranged in a brucite-like layer. Even if the full width at half height, close to 0.3° (2θ), is smaller, the lateral coherence inside the layers, around 30 nm, is also poor. Changing the nickel source with nitrate yields a similar result as far as the crystallinity is concerned, whereas the use of nickel chloride does not yield any crystallised phase. The same absence of reaction is evidenced when starting from a suspension of nickel hydroxide. Another possibility to improve crystallinity is to increase the fluorine ratio. However, it has been noticed that too much fluorine promotes the Si–C bond breaking in the alkoxide. For instance, 85% Si–C bonds are broken when F/Si = 2 as evidenced by the N chemical analysis value. The resulting silicate always presents a similar XRD diagram but with a (001) reflection lowered to 14 Å.

From the XRD patterns, it can therefore be proposed that nickel ions build up structural units similar as the one observed in $Ni(OH)_2$, *i.e.* edge sharing octahedra forming infinite layers, in relation with the presence of 2.67 and 1.54 Å diffraction lines, separated from each other by an interlayer distance of 21 Å. The photoelectron spectrum is in agreement with such an environment; in particular, the occurrence of a "shake up"[9] structure after the $2p_{1/2}$ and $2p_{3/2}$ peaks confirms this point. Furthermore, the UV–vis spectrum reveals two broad absorption bands at 410 and 700 nm as expected for oxygen coordinated nickel ions.[10]

The preferred orientation can be enhanced by film deposition. The powder is first dispersed in aqueous media leading to a colloidal suspension; second, settling combined with water evaporation upon room temperature yields films on different substrates (glass, metals). Only (00*l*) reflections are observed. It is then possible to obtain thick films of these silicates (up to several microns). The (*hk*0) lines disappear on the film diffractogram (Fig. 2), proof of its good texture.

Chemical analysis

The chemical analysis results are collected in Table 1.

For samples 2 and 3, oxygen content is deduced from the other percentages. The first feature concerning these analyses is that the Ni : Si ratio, around 3 : 2, is different from the 3 : 4 value expected from the initial conditions. The extra silicon remains in the filtrates as oligomeric or soluble species. The second feature is related to the Si–C bond stability in our experimental conditions with similar atomic contents for Si and N, almost every silicon atom bearing an aminopropyl chain. The last point concerns the nature of the group around nitrogen: is it NH_2 or NH_3^+? pH measurements show that the addition of (aminopropyl)triethoxysilane in an aqueous solution of nickel acetate and ammonium fluoride leads to an increase of the pH from 6.5 to 7.5 and further decrease to 7 after equilibrium is reached. In this pH range, propylamine is protonated since its pK_a is close to 11. We can consider that the acid–base equilibrium constant of APTES is not very far from the value of propylamine. Therefore, the formulae have been written by considering the presence of NH_3^+ groups. In order to balance charge, the presence of acetate groups (evidenced by IR see below) as counter anions has been taken into account. Moreover, we also included water molecules as observed by thermal analysis and IR spectroscopy yielding the following results:

Sample 1: $Ni_3Si_{2.07}(C_3H_6NH_2)_{1.89}(CH_3COO)_{2.88}O_{5.13}(OH)_{1.14}\cdot 1.8H_2O$

Sample 2: $Ni_3Si_{2.13}(C_3H_6NH_2)_{1.98}(CH_3COO)_{2.25}O_{5.28}(OH)_{1.05}F_{0.69}\cdot 1.76H_2O$

Sample 3: $Ni_3Si_{2.31}(C_3H_6NH_2)_{2.1}(CH_3COO)_3O_{3.96}(OH)_{3.69}F_{0.63}\cdot 2H_2O$

Table 1 Chemical analysis for hybrid nickel silicates

Sample	Ni	Si	F	C	N	H	O
1 Obs.	27.01	8.92	—	21	4.06	5.18	33.94
1 Calc.	27.11	8.95	—	21.11	4.07	4.68	34.07
2 Obs.	27.88	9.43	2.14	19.72	4.4	4.59	31.84
2 Calc.	27.84	9.46	2.07	19.80	4.38	4.61	31.84
3 Obs.	24.65	9.1	1.69	20.68	4.15	4.74	34.99
3 Calc.	24.60	9.06	1.67	20.62	4.11	4.97	34.97

Thermal analysis

The thermal decomposition under air of the hybrid silicate (sample 2) is illustrated in Fig. 4. Total weight losses of 44.3, 46.4 and 46.5% are observed for samples 1, 2 and 3, respectively. These values slightly differ from the values deduced from chemical analysis (46.6, 44.4 and 49.2% respectively), but are strictly reproducible. Three steps occur during the treatment: up to 150 °C, water molecules are desorbed, followed by the departure of 15% of the acetate groups present in the compounds (Fig. 4b, inset). Finally, from 250 °C to 500 °C, the amine moieties and the rest of the acetate, detected by mass spectroscopy, are totally decomposed, yielding a concomitant strongly exothermic effect. The final compound corresponds to a mixture of NiO and amorphous SiO_2 under air and Ni and amorphous silica under argon. The water content (around 5%) has been calculated from the TGA trace as the weight loss below 150 °C, the temperature where mass 60 species start to be detected by mass spectrometry.

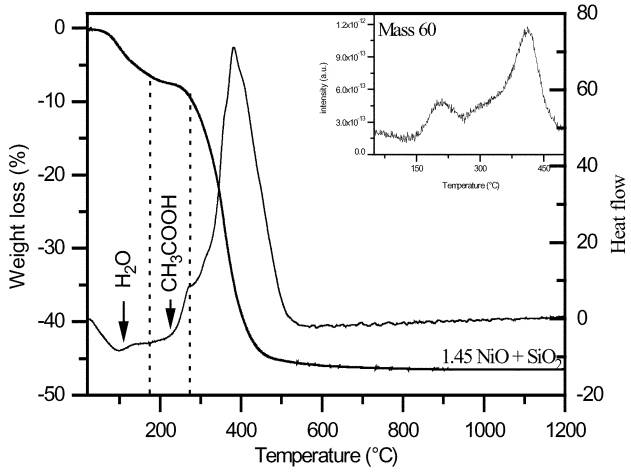

Fig. 4 TG–DTA curves for sample 2. Inset: mass spectroscopy curve for the mass 60 relating to CH_3COOH.

IR Spectroscopy

The IR spectrum of the compounds with fluorine (Fig. 5a) reveals, first, the presence of a sharp and intense band at 3627 cm^{-1} which corresponds to the ν(O–H) stretching mode and is characteristic of free hydroxy groups, *i.e.* groups not involved in hydrogen bonds. Such a band is also evidenced in β-$Ni(OH)_2$[11] and also in phyllosilicates.[12] Therefore, as already expected from the X-ray diffraction pattern, it can be concluded that the nickel ions are inserted in a brucite-like layer. On the other hand, such a band does not appear for the compound without fluorine, suggesting the presence of hydrogen bonds by means of anions and/or water molecules for instance. This observation was also done for α-$Ni(OH)_2$ samples.[11] The broad band at around 3300 cm^{-1} is related to bonded OH groups, but its intensity is quite low. Water is evidenced by the band at 1642 cm^{-1}.

The inorganic framework is also evidenced by the broad band of the Si tetrahedron vibrations with a maximum at 987 cm^{-1} and shoulders at 915, 1049, 1132 and 1190 cm^{-1}.[1,13,14] Whereas the band at 1132 cm^{-1} disappears after thermal treatment at 250 °C (Fig. 5b), the other ones are unaffected. Moreover, the band at 1190 cm^{-1} can be attributed to the Si–C vibration band. An IR spectrum has also measured on a gel obtained by hydrolysis–condensation of APTES. It reveals (Fig. 5c) that the band related to silicate groups is shifted towards higher wavenumbers, with two intensity equivalent components at 1030 and 1132 cm^{-1}.

The aminopropyl chain is evidenced through its N–H vibration bands, ν at 3290 cm^{-1} and δ at 1560 cm^{-1}, C–N at 1294 cm^{-1} as well as through its CH_2 vibration bands as reported in Table 2. The broad bands at 3086 and 2160 cm^{-1} could be related to the presence of protonated amine, which formation is expected from the pK_a and pH values. After reaction with *p*-nitrobenzaldehyde, an imine is formed as evidenced from the corresponding IR spectrum (Fig. 5d) which shows a band at 1654 cm^{-1} attributed to imine vibration and the asymmetric and symmetric stretching vibrations of the nitro group at 1518 and 1341 cm^{-1}, respectively.[15] Moreover, the XRD diffractogram (not shown) reveals the shift of the (001) peak towards higher values from 21 to 23 Å.

As written in the formulae, acetate ions are also present in the compounds and have been evidenced by coupling thermal analysis and mass spectroscopy: the weight loss between 150 and 250 °C is due to the departure of acetic acid (mass 60).

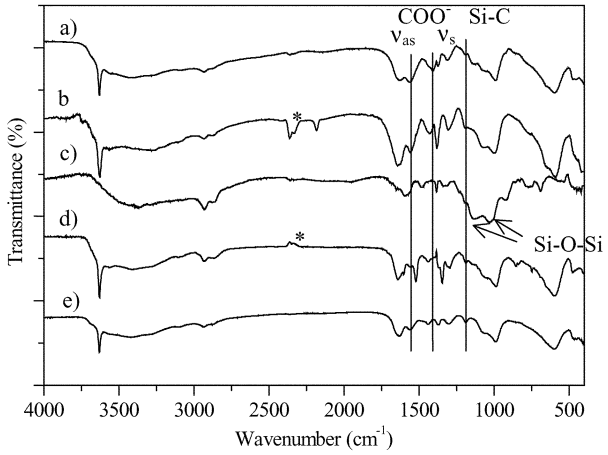

Fig. 5 FTIR spectra for: (a) sample 2; (b) sample 2 heated at 250 °C under air; (c) a gel obtained from $Si(OC_2H_5)_3(CH_2)_3NH_2$ under the following conditions: a water and ethanol mixture in 3 : 2 ratio is added to a solution of $Si(OC_2H_5)_3(CH_2)_3NH_2$ in ethanol (1 : 4). The gelation occurs within 2 hours, under HNO_3 catalysis; (d) compound obtained from the reaction between hybrid silicate of nickel and *p*-nitrobenzaldehyde in dried methanol at 60 °C; (e) sample 2 treated with a NaOH solution.

Table 2 Recapitulation of the band assignment for the FTIR spectra

Band vibration (cm^{-1})	Assignment	Reference
3627	ν (NiO–H)	11
3290	ν (N–H)	15
3086, 2160	ν (NH_3^+), ν (NH_3^+)	15
2929, 2875,	ν (CH_2)	15
1435, 1371, 1303	δ (CH_2), ω (CH_2)	15
1642	δ (H_2O)	
1560	ν_{as} (CH_3COO^-)	
1406	ν_s (CH_3COO^-)	
1294	C–N	13
1190, 770 (sh)	Si–C	
1049, 987	Si–O–Si	
915 (sh)	Si–OH	
607	Ni–OH	

Moreover, acetate ions are characterised by the COO^- antisymmetric (1560 cm^{-1}) and symmetric (1406 cm^{-1}) stretching vibration bands.[16] After thermal treatment at 250 °C, the ν_s band disappears and the other band decreases (Fig. 5b). As δ (N–H) appears in the same region, a band is still visible at the 1560 cm^{-1} position. This evolution has been related to the loss of acetate ions.

On the spectrum of the sample treated at 250 °C (Fig. 5b), three bands clearly appear at 2358, 2324 and 2160 cm^{-1}. Whereas the first two can be related to atmospheric CO_2 (labelled by * in Fig. 5) and are also present in the spectrum of the starting materials, their intensities are too high to be only of this origin. The third band can be attributed to CO. The concomitant presence of both CO and CO_2 trapped in the compound is probably related to the acetate decomposition.

In order to get more insight into the IR characterization, the samples have been reacted with a NaOH solution to promote the acetate exchange by OH^- ions. The corresponding spectrum (Fig. 5e) reveals the disappearance of the 1406 cm^{-1} ν_s acetate vibration band as well as of the band at 1132 cm^{-1}, bands that also disappeared after 250 °C thermal treatment. Moreover, the bands related to the aminopropyl group are clearly evidenced and the water band is stronger, as confirmed by the corresponding TGA result. A similar XRD pattern is obtained after NaOH solution treatment, with a shift of the (00*l*) peaks towards lower distances, approximately 1 Å difference.

XAS results

The $k\chi(k)$ absorption coefficient is plotted in Fig. 6a for the different samples. The Fourier transform of the EXAFS oscillations presents two main peaks (Fig. 6b). The first one at 1.6 Å (not corrected for phase shift) can be attributed to the first next nearest neighbours of Ni, which are 6 oxygen atoms in an octahedral coordination. Subsequent fitting of the inverse Fourier transform of this peak with calculated phase and amplitude obtained from $Ni(OH)_2$, or $Ni_3Si_2O_5(OH)_4$ leads to 6 oxygen atoms at 2.04(5) Å.

The second peak of the Fourier transform of the EXAFS oscillations was fitted using the calculated phase and amplitude of $Ni_3Si_2O_5(OH)_4$. We found that a Si contribution has to be taken into account to match the inverse Fourier transform of the second peak, as shown in Fig. 7. Results for the different materials are collected in Table 3. The best fit was obtained by taking into account 6 Ni at 3.11(5) Å and 2 Si at 3.25(5) Å.

Magnetic measurements

The compounds present a paramagnetic–ferromagnetic transition below 20 K. Magnetic data are collected in Table 4. The susceptibilities (recorded under 100 Oe) are fitted to a classical Curie–Weiss law in the 100 to 300 K range, with $\chi = C/(T - \theta)$ where $C = Ng^2\mu_B^2S(S + 1)/3k$, assuming a spin only equation

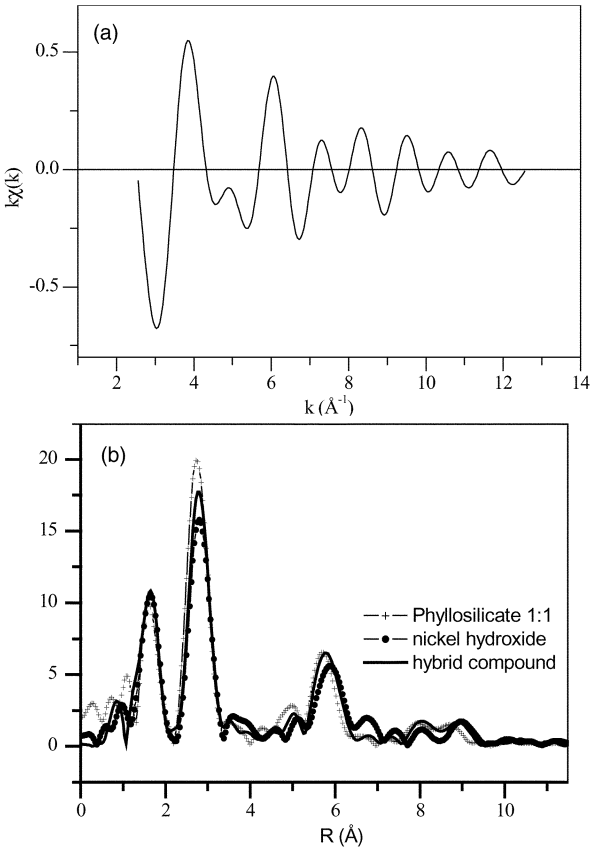

Fig. 6 (a) Experimental $k\chi(k)$ for sample 2. (b) Experimental Fourier transforms of both references and hybrid compound (NH_4F).

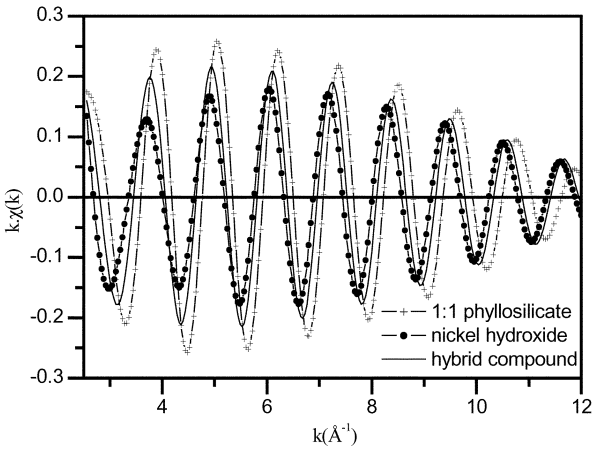

Fig. 7 Filtered second FFT peak of both references and hybrid compound (NH_4F).

with $S = 1$, for nickel, is the Curie constant. The positive θ values indicate ferromagnetic interactions in the compounds. The Landé factors can be calculated from the above equation and range from 2.0 to 2.2 which is an expected value for Ni^{2+} in octahedral coordination.

Magnetisation *versus* applied field at 2 K (Fig. 8) exhibits a hysteresis with coercive fields close to 3000 Oe depending on the samples. Magnetisation in a 5 T applied field reaches 1.5 μ_B mol^{-1} Ni^{2+} *versus* 2 μ_B mol^{-1} Ni as expected for Ni^{2+}, in an octahedral configuration. It has to be noticed that the saturation does not seem to be reached at 5 T. The ac susceptibility (Fig. 9) allows us to confirm the paramagnetic–ferromagnetic transition evidenced as a sharp peak for both the in-phase and out-of-phase components of the complex

Table 3 Results of the fit procedure using phase and amplitude extracted from FEFF6 of 1 : 1 phyllosilicate

	N		R ($\pm$0.05)/Å	σ/Å	ρ
Hybrid sample (NH_4F)	O	6	2.04	0.068 (2)	0.057
	Ni	6	3.11	0.075 (2)	
	Si	2[a]	3.25	0.030 (5)	
Without F^-	O	6	2.04	0.075 (2)	0.061
	Ni	6	3.11	0.077 (2)	
	Si	2[a]	3.23	0.051 (5)	
HF	O	6	2.04	0.069 (2)	0.063
	Ni	6	3.10	0.079 (2)	
	Si	2[a]	3.24	0.036 (5)	

[a]During the procedure fit, N_{Si} varied between 1.9 and 2.1 for all hybrid compounds without any changes in the fit result. So we set N_{Si} to 2 in this table.

Table 4 Magnetic data for the three samples

	T_C/K	C/emu mol^{-1} K	g	θ/K	H_c/Oe at 2 K
Sample 1	18	1.21	2.2	37	3800
Sample 2	15	1.14	2.1	31	3100
Sample 3	16	0.98	2.0	36	2700

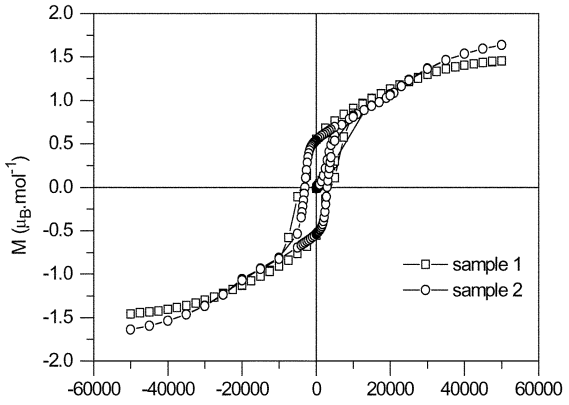

Fig. 8 Magnetisation *versus* applied field at 2 K for samples 1 and 2.

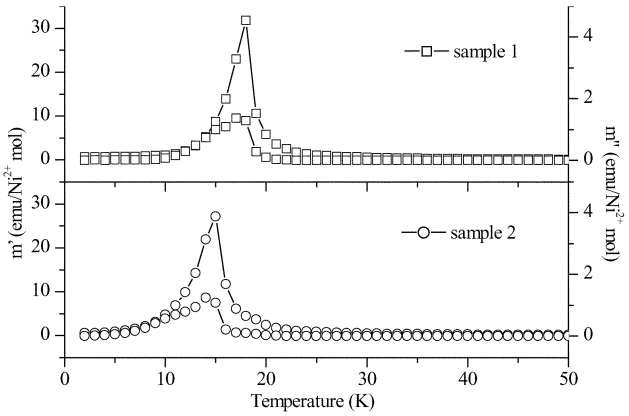

Fig. 9 AC susceptibilities for samples 1, 2 and 3.

susceptibility, as expected for a material displaying long range magnetic ordering.

Discussion

Hydrothermal reaction between nickel acetate and (aminopropyl)triethoxysilane in the presence or absence of fluorine ions (HF or NH_4F) yields the reproducible formation of a lamellar

compound with an interfoliar distance of 21 Å. Many attempts have been made to try to increase the crystallinity. However, the variation of some experimental conditions is restricted by secondary reactions: higher temperatures promote Si–C breaking, the same result if the fluorine ion concentration is increased. Using OH^- ions as mineraliser or increasing the reaction time or introducing already prepared sample as seeds does not improve the crystallinity. It has to be mentioned that hydroxysilicates rarely reveal a high crystallinity.

Before hydrothermal treatment, we never observe the formation of nickel amine complexes with their characteristic blue colour; in our case, the suspension is always green. Furthermore, the UV–vis spectrum of the lamellar compounds reveals two absorption bands at 400 and 700 nm as expected for oxygen coordinated nickel ions.[10] A different result is observed when the alkoxysilane is functionalised by a diamine.[6,16] In this case, two alkoxide molecules provide an appropriate geometry to promote the complex formation. However, further hydrothermal treatment destroys the amine complexes yielding oxygen coordinated nickel.[6]

Chemical analysis allows us to propose formulae. However, some discrepancies appear between chemical and thermal analysis, particularly for sample 3. On the other hand, very similar and reproducible weight losses are measured for samples 2 and 3, samples also exhibiting nearly the same basal spacing, 20.8 and 21 Å, respectively. Taking into account these results, we deduce the formation of a unique phase where all silicon atoms bear a propylammonium chain, the NH_3^+ charge being balanced by acetate groups. From the corresponding formulae, one can observe that the compounds look like 1 : 1 phyllosilicates. However, to explain the interfoliar distance, silicon atoms must be bonded to both sides of the brucite layer.

The low crystallinity precludes any precise structure determination and other techniques have been used to propose a structural model.

X-Ray absorption spectroscopy confirmed that Ni cations are arranged in a hydroxide-like layer. The fit of the first shell is in agreement with an octahedral oxygen environment and the second shell is well fitted with 6 Ni at a distance compatible with such a layer. Moreover only such a framework can lead to the 2.67 and 1.54 Å diffraction peaks which correspond to two perpendicular Ni–Ni intralayer distances.

IR spectroscopy also reinforces the proposed presence of a brucite-like layer with the presence of a sharp vibration band at 3627 cm^{-1}, a band already mentioned in β-$Ni(OH)_2$ as well as in phyllosilicates. Moreover, UV spectroscopy confirms that Ni^{2+} ions are only oxygen bonded.

Another proof that Ni^{2+} ions are arranged in octahedral sites sharing edges is the occurrence of 3D ferromagnetic ordering as previously reported.

For 3D mean field type compounds the Curie temperature is defined as the highest temperature at which the out-of-phase component is non-zero and correspondingly the temperature at which the in-phase component is at a maximum. However, the peak in the in-phase susceptibility is not coincident with the temperature at which the out-of-phase component is non-zero; we define the Curie temperature at the maximum point of the in-phase susceptibility.

This may be interpreted as being due to the two-dimensional nature of the compound. Accordingly there is a range of temperatures where the correlation length within the plane increases exponentially before long range ordering takes place. This 2D correlation results in a non-linearity of the susceptibility and therefore a weak and observable out-of-phase component before the transition.

It has already been mentioned that for 13 Å separated layers without chemical bonds, direct exchange coupling is too small to explain 3D ferromagnetic order. It seems reasonable to also propose dipolar interaction between 21 Å separated layers to be responsible for the magnetic ordering.

For compounds obtained by precipitation using (aminopropyl)triethoxysilane, several authors proposed a structural model deriving from phyllosilicates. This configuration implies that every corner of the SiO_4 tetrahedron is shared. In the case of organically modified alkoxides, only 3 oxygen ions are available for corner sharing. Thus the formation of hexagonal SiO_4 rings is not possible as the Si–C bond can not be shared. XRD evidences a lamellar structure as shown by the observed (00*l*) planes which intensity strongly increases on films.

Chemical analysis and IR spectroscopy data confirm the presence of an aminopropyl chain bonded to silicon with very similar observed Si and N contents and the observation of a Si–C vibration as well as the vibrations related to C–H, C–N and N–H bonds.

The remaining question concerns the existence of a link between the silicon groups and the brucite layer. First, the observation of reproducible XRD patterns with a 21 Å interlayer distance together with a constant Ni : Si indicates a regular stacking of the previous components. Second, this conclusion is strongly reinforced by the EXAFS results, with a Si contribution in the second peak of the Fourier transform of the oscillations. These results can thus allow us to show that the silicate entities are mixed with the brucite-like layers at the molecular level, forming a hybrid organic–inorganic compound. Third, IR spectroscopy evidences a shift towards lower wavenumbers of the Si–O vibration bands as well as a strong modification of the relative intensities in the samples compared to a gel obtained by hydrolysis polymerisation of APTES. In particular, only one main vibration is observed compared to the two presented by the polymeric APTES gel. Therefore, the hypothesis of a gel-like silicon network trapped between brucite-like layers can be eliminated.

As written in the general formula, acetate ions are present in the compounds and are characterised by the bands at 1560 and 1406 cm^{-1}. We suggest that acetate ions are linked to the ammonium group *via* hydrogen bonding. The formation of such hydrogen bonds to stabilise the structure could explain why the compounds can be obtained starting from nickel acetate or nitrate and not in the case of chloride, where Cl is a less good acceptor for hydrogen bonds. The delocalisation of the hydrogen bond from the nitrogen of RNH_3^+ towards the oxygen of the acetate can explain the observed reactivity with *p*-nitrobenzaldehyde to give rise to an imine.

On the one hand, when regarding the chemical analysis, acetate is present in higher quantities than amine and on the other hand, from TGA experiments, two kinds of acetate ions are evidenced, leading to one loss at 150 °C and another close to 400 °C. Some of them are probably adsorbed on the surface of the particles, explaining the strong smell of acetic acid. It is difficult to experimentally ascertain but we can not exclude that some of the acetates are in interaction with Ni^{2+} through the formation of a bond similar to the one observed in hydroxyacetate.

Finally, our description would be preferentially based on the grafting of low-molecular-weight silane entities, formed in aqueous solution, to $Ni(OH)_2$ brucite layers as it is illustrated in Fig. 10. Such a geometry can explain the Ni/Si stoichiometry obtained.

Conclusion

Hydrothermal synthesis between nickel acetate and APTES with or without F^- ions (HF or NH_4F) yields the reproducible formation of a hybrid organic–inorganic compound where silicon atoms are grafted on a brucite-like layer containing nickel ions. The amine function is still accessible to further reaction as shown with the formation of an imine by reaction

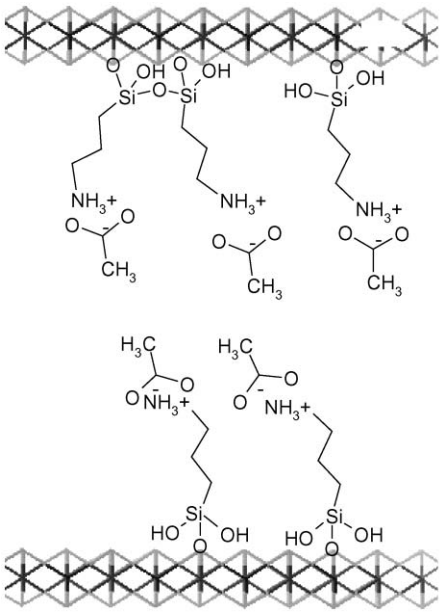

Fig. 10 Proposed structure for obtained hybrid nickel silicates.

with *p*-nitrobenzaldehyde. In the same manner acetate ions can also be exchanged by other anions exhibiting optical properties for instance. The hybrid compound can therefore be a source for new materials combining both magnetic and optical properties. Such studies are in progress.

Acknowledgement

The experimental XAS records were performed with the assistance of Dr Stuart Ansell at ESRF. The authors are indebted to Dr Agnès Traverse at LURE (French synchrotron) for fruitful advice concerning XAS analysis and fitting.

References

1 See for example *Chem. Mater.*, 2001, **13**, issue 10.
2 N. T. Whilton, S. L. Burkett and S. Mann, *J. Mater. Chem.*, 1998, **8**, 1927.
3 S. L. Burkett, A. Press and S. Mann, *Chem. Mater.*, 1997, **9**, 1071.
4 Y. Fukushima and M. Tani, *Bull. Chem. Soc. Jpn.*, 1996, **69**, 3667.
5 M. G. da Fonseca and C. Airoldi, *J. Chem. Soc., Dalton Trans.*, 1999, 3687.
6 M. Richard-Plouet and S. Vilminot, *J. Mater. Chem.*, 1998, **8**, 131.
7 A. Michalowicz, EXAFS Signal Treatment and refinement programs, LURE, Orsay, France. Available on http://www.LURE.fr.
8 J. J. Rehr, J. Mustre de Leon, S. I. Zabinsky and R. C. Albers, *J. Am. Chem. Soc.*, 1991, **113**, 5135.
9 A. N. Mansour, *Surf. Sci. Spectra*, 1996, **3**, 255.
10 F. A. Cotton and G. Wilkinson, *Advanced Inorganic Chemistry*, 5th edn., Wiley Interscience, New York, 1988.
11 C. Tessier, L. Guerlou-Demourgues, C. Faure, A. Demourgues and C. Delmas, *J. Mater. Chem.*, 2000, **10**, 1185.
12 S. W. Bailey, in *Reviews in Mineralogy, Hydrous Phyllosilicates*, ed. S. W. Bailey, Mineralogical Society of America, Washington, 1988, vol.19, p. 243.
13 D. G. Kurth and T. Bein, *Langmuir*, 1995, **11**, 3061.
14 C. Chiang, H. Ishida and J. L. Koenig, *J. Colloid Interface Sci.*, 1980, **74**, 2.
15 N. B. Colthup, L. H. Daly and S. E. Wiberley, in *Introduction to Infrared and Raman Spectroscopy*, Academic Press, San Diego, 1990, 3rd edn.
16 K. Nakamoto, *Infrared and Raman Spectra of organic and coordination compounds*, 4th edn., Wiley-Interscience, New York, 1986.
17 A. Kaiser, C. Görsmann and U. Schubert, *J. Sol–Gel Sci. Technol.*, 1997, **8**, 795–799.